

# Grayscale lithography for chiral nanophotonic structures

*Jefferson Dixon, Michelle Solomon*

*SNF staff mentor: Swaroop Kommera*

*External mentor: Andrew Ceballos*

## **Introduction**

Subwavelength periodic structures (*i.e.* metamaterials) offer the opportunity to manipulate light at the nanoscale to achieve arbitrary beamsteering, asymmetric transmission, and locally enhanced light-matter interactions. Metamaterial structures that are not superimposable with their mirror image (*i.e.* chiral structures) discriminate between different polarizations of light by virtue of their asymmetry, leading to polarization-selective light transmission.<sup>[1]</sup> Silicon is an ideal candidate for such a metamaterial due to its transparency at telecommunication frequencies. However, fabricating structures that exhibit three-dimensional chirality requires breaking out-of-plane symmetry, which necessitates that the silicon structure be of non-uniform height, posing a unique fabrication challenge.

The proposed silicon metamaterial structure achieves the desired three-dimensional chirality by fabricating a hole with three steps of varying height. The grayscale lithography capability of the Heidelberg MLA 150 is well suited to fabricate a large array of these structures, wherein the grayscale exposure determines the depth of each step after etching. We describe using the Heidelberg MLA 150 to etch a 25x25 array of 10  $\mu\text{m}$  and 5  $\mu\text{m}$  holes that exhibit chiral symmetry, exploring patterning and etching near the resolution limit of the Heidelberg.

## **Determining dose for grayscale patterning**

### ***Contrast curves for Shipley 3612 photoresist***

Contrast curves describe the level of resist removed after development as a function of exposure dose. At low doses, minimal to no resist is exposed and therefore no resist is removed during development. Dose-to-clear is defined as the exposure dose that corresponds to all resist being removed after development. Any dose between these two points can be used for grayscale patterning, as the resist will be partially exposed. The contrast curve for Shipley 3612 photoresist is given in Figure 1.

For 1  $\mu\text{m}$  of Shipley 3612 resist, grayscale exposure is observed between 15 and 40  $\text{mJ}/\text{cm}^2$ , with 40  $\text{mJ}/\text{cm}^2$  beginning the dose-to-clear. Similarly, 1.6  $\mu\text{m}$  of 3612 resist exhibits grayscale exposure between 15 and 50  $\text{mJ}/\text{cm}^2$ , and 50  $\text{mJ}/\text{cm}^2$  is the dose-to-clear. As expected, thicker resist allows for a larger range of grayscale exposure. For the remainder of this work we consider 1  $\mu\text{m}$  of 3612 photoresist for consistency and to further enable resolution-limited patterning.

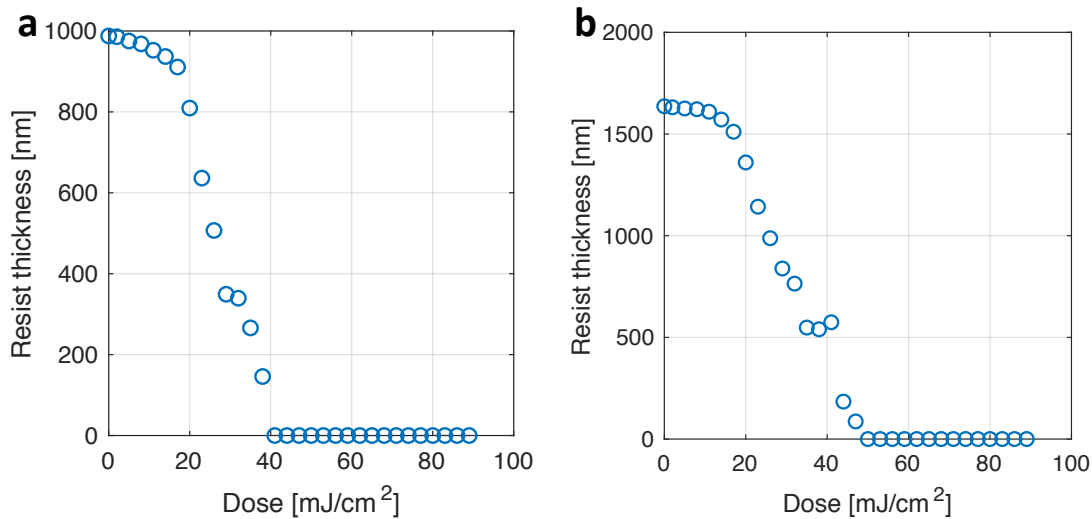


Figure 1. Contrast curves for Shipley 3612 resist. The resist was coated using svgcoat at (a) 1  $\mu\text{m}$  and (b) 1.6  $\mu\text{m}$  thicknesses, developed in svgdevelop and measured by Nanospec. Error tolerance is  $<100$  nm.

### ***Pattern abnormalities in under- and over-exposed features***

There are several factors to consider when determining the exposure dose, especially for patterns with features below 10  $\mu\text{m}$ . One should consider the sidewall characteristics of the exposure, how the feature geometry may change when under- or over-exposed (as grayscale lithography necessitates), and how the dose-to-clear value may change if the features are sufficiently small or close together. We have already discussed the dose-to-clear value shift for features  $<10$   $\mu\text{m}$ , so we redirect our attention towards the sidewall characteristics after exposure. As observed in Figure 2, the sidewall profile changes dramatically as the exposure dose increases. At low doses, the sidewall is heavily sloped which becomes especially apparent for small features. For a circle exposed nominally at 2  $\mu\text{m}$ , the sidewall can easily extend 500 nm into the pattern from all sides, as seen in Figure 3. However, overexposing the pattern corrects this behavior and the sidewalls become more vertical.

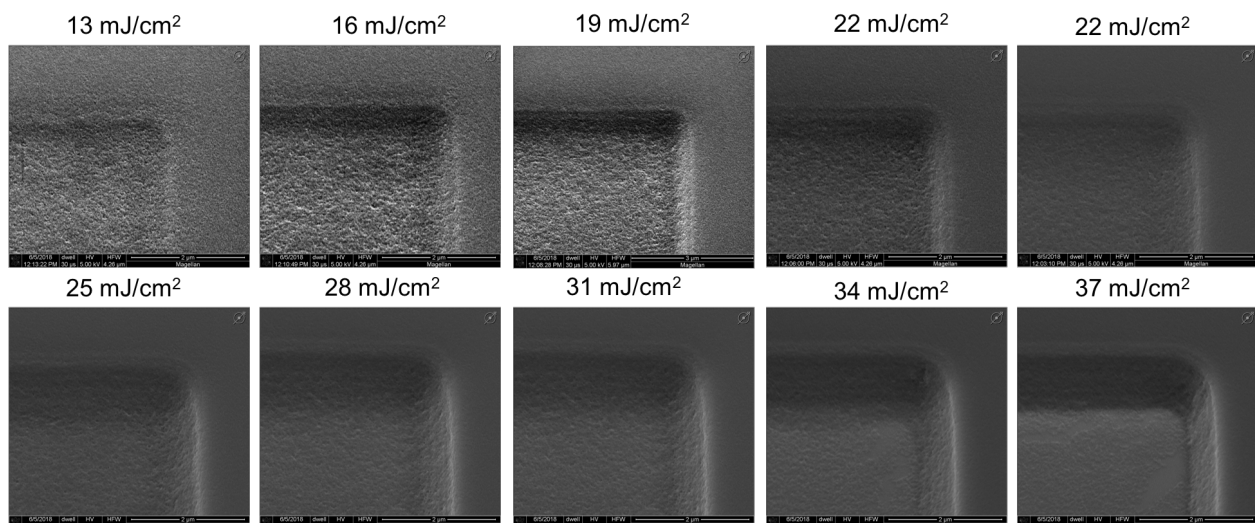


Figure 2. Sidewall profiles of 1  $\mu\text{m}$  3612 photoresist after exposure and development (coated in 3 nm Au). As the dose approaches dose-to-clear, the sidewalls become observably more vertical.

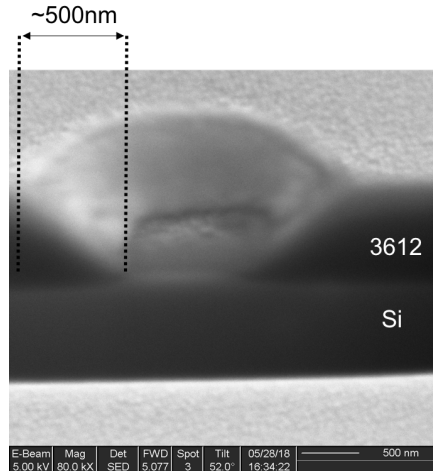


Figure 3. Cross section of 2  $\mu\text{m}$  diameter (nominal) circle pattern in photoresist prior to etching (coated in 5 nm Au). The sidewall extends  $\sim 500$  nm into the pattern for a dose of  $\sim 30$   $\text{mJ}/\text{cm}^2$ .

### ***Dose scaling as a function of feature size***

It should be noted that as feature sizes decrease below 10  $\mu\text{m}$ , the contrast curve shifts slightly to the right. Dose-to-clear for a 10  $\mu\text{m}$  pattern may be 40  $\text{mJ}/\text{cm}^2$ , but will likely be closer to 45  $\text{mJ}/\text{cm}^2$  for 1  $\mu\text{m}$  features. Figure 4 depicts post-development circular apertures (note: no descum process was performed on these samples), showing both the sidewall characteristics of grayscale features and the shift in dose-to-clear as dimensions decrease. We clearly observe the parabolic “well” shape of underexposed features, owing to the significant slope of the sidewalls and the gaussian-type exposure of photolithography.

The effects of under- and over-exposure on the etched geometry is discussed further in the etching section of this document.

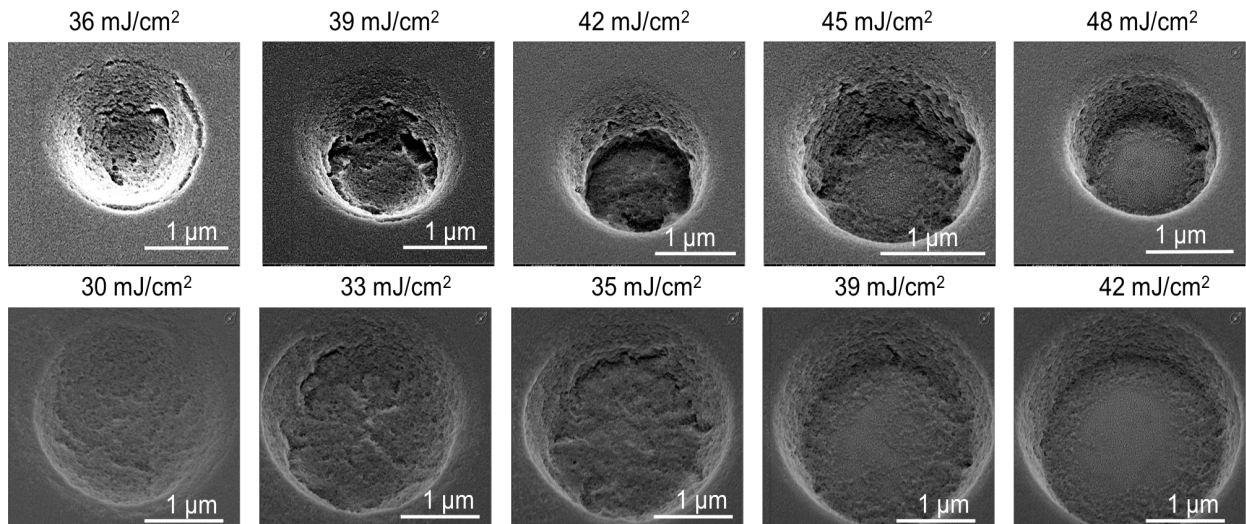


Figure 4. Circle pattern in photoresist prior to etching (coated in 5 nm Au). Top row: 2  $\mu\text{m}$  diameter circle exposed at 36-48  $\text{mJ}/\text{cm}^2$ ; Bottom row: 3  $\mu\text{m}$  diameter circle exposed at 30-42  $\text{mJ}/\text{cm}^2$ . As the dose increases, the exposed pattern becomes more anisotropic with the sidewalls becoming more vertical; this is especially noticeable in smaller features.

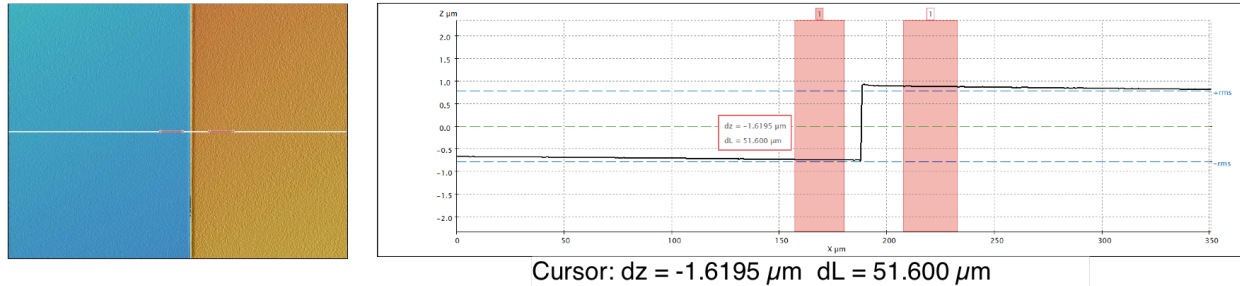


Figure 5. S-neox thin film measurement of 1.6  $\mu\text{m}$  of 3612 photoresist.

### **Sensofar S-neox for measuring transparent films**

The Sensofar S-neox is a 3D optical profiler that acquires film thickness information using interferometry and has the added benefit of being able to scan large areas quickly and export a 3D image of the sample profile. However, its use on transparent films, such as Shipley 3612 photoresist, is not documented. Figure 5 presents the result of measuring film thickness of a pattern in 1.6  $\mu\text{m}$  of 3612 photoresist. The S-neox consistently measured film thickness to within 100 nm of Nanospec interferometry measurements, with a unique exception: When measuring height variation, the S-neox may measure from the surface of the substrate to the next step in height or measure from the top of the resist to the next step in height. Therefore, if the pattern is such that the step is from 0.5  $\mu\text{m}$  of resist to 1.5  $\mu\text{m}$  of resist, it may measure this as a 1  $\mu\text{m}$  step or 0.5  $\mu\text{m}$  step (i.e.  $1.5-0.5=1$  or  $0.5-0=0.5$ ). The scan variation in z-height is much larger than the thickness of the resist, and the silicon substrate is more reflective than the resist surface, which causes the S-neox to choose between taking the silicon surface as its reference point or the film surface as its reference point. This may be tuned by using different illumination conditions. We conclude that the S-neox is capable of transparent film measurements, albeit with a reliability less than that of the Nanospec interferometer.

### **Etch processing optimization**

All of the etched samples were processed with a Lam Research 9400 TCP Poly Etcher (lampoly) using just the breakthrough etch step, which uses 100 sccm  $\text{C}_2\text{F}_6$ . This chemistry etches silicon and resist with a nominally one-to-one selectivity with respect to resist. The etch rate is approximately 177 angstroms/10 s. The resist on these samples prior to exposure was 1  $\mu\text{m}$  thick.

### **Bake and descum processing**

Optimization of the bake and descum processes prior to the etch is critical to good pattern transfer from resist to the underlying silicon substrate. After exposing, developing, and baking for one minute on a 110°C hotplate, significant grass formed at low doses where the resist had not been fully exposed. At higher doses, as can be seen in Figure 5c, extremely rough sidewalls were observed. Even though the center of the circles here have reached dose-to-clear, as evident by the smooth surface of the silicon, resist “scum” was left over near the edges of the wells, leading to this roughness.

In order to remedy the grass and rough sidewalls, we first used a “descum” process, which removes a small amount of resist in order to even out the surface of the sample before etching.



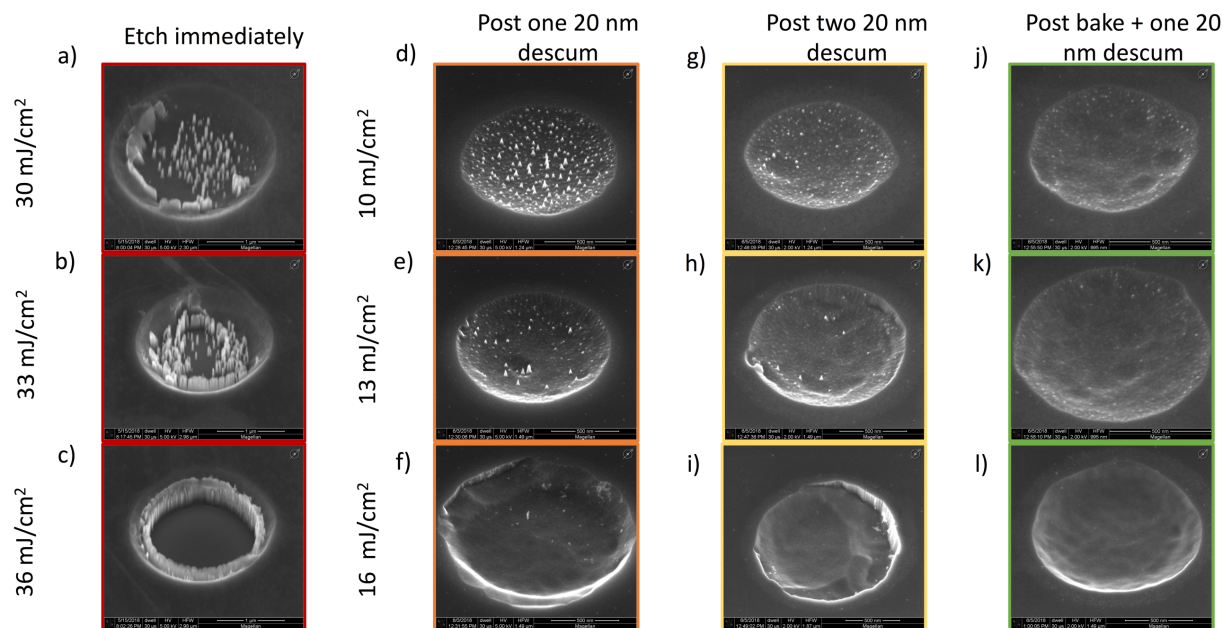


Figure 6. Transfer of exposed pattern into silicon after etching for nominally  $2\ \mu\text{m}$  diameter circles. a)-c) were exposed with 30-36  $\text{mJ}/\text{cm}^2$ , and etched for 420 s immediately after development (including a one minute bake on a hot plate), d)-f) were exposed with 1

Figure 6 shows decrease in grass height for the lowest dose circles, as well as decreased roughness on the sides of the circles for the higher dose circles, despite the fact that the doses used here are much lower than in a-c. Figure 6 shows an improvement with a second descum step added, although some small grass is still visible for the lowest dose, and the sidewalls are not evenly etched around the perimeter of the circles. The results from our optimized process are shown in Figure 6, which were attained after a 2 hour bake in a  $110^\circ\text{C}$  oven in addition to one 20 nm descum process. Here, we see no full-sized grass at the lowest doses, although there is still some slight roughness to the surface. At the higher doses, we observe a smoothing-out of the sidewalls and an even etch.

### **Diameter vs. Dose Curves**

In addition to topological differences in the resist, we found that different doses also led to different diameters in our circles, even when we expose the same diameter pattern. This is shown in Figure 7, which plots the measured etched diameter for 2, 3 and 5  $\mu\text{m}$  circles, across a wide range of doses. All of these samples were etched for 200 s using the breakthrough recipe in lampoly, described above. We note, in particular, that below dose-to-clear for each size, the diameter is generally less than the nominal diameter, mainly due to the angled sidewalls. As the structures are etched further, we would expect this discrepancy from the nominal diameter to become less pronounced. As dose approaches dose-to-clear, marked by vertical dotted lines in Figure 6, the diameter of the circles reaches the diameter of our pattern, indicated on the plots by horizontal dotted lines. As the dose is increased past this point, the diameter of the structures continues to increase, likely due to overexposure. The diameter appears to saturate as we reach 80-90  $\text{mJ}/\text{cm}^2$  for the 2 and 5  $\mu\text{m}$  circles.

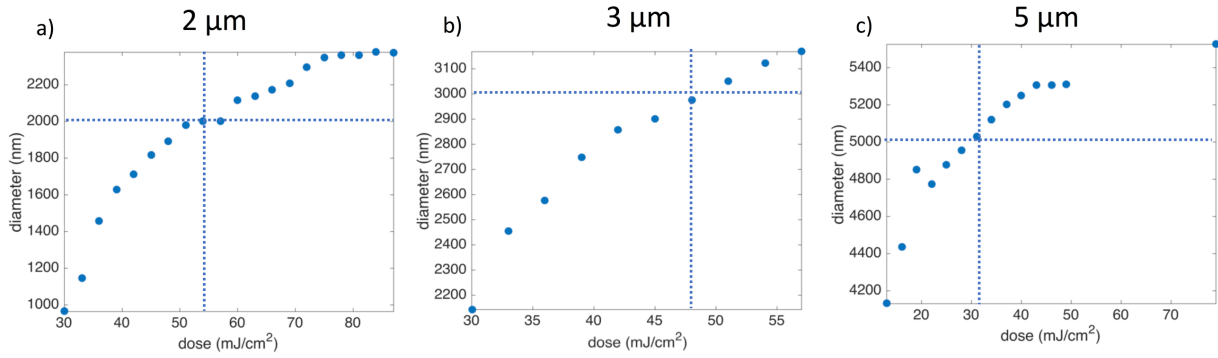


Figure 7: As the dose is increased, the diameter of the etched circles changes. This can be seen in for a) 2  $\mu\text{m}$ , b) 3  $\mu\text{m}$ , and c) 5  $\mu\text{m}$  nominally exposed circles. Horizontal lines indicate nominal diameter of exposed structures and vertical lines indicate dose-to-clear.

### ***Difference in dose-to-clear evident post etching***

As quantified in Figure 6, the dose-to-clear varies depending on the size of the structure. This is qualitatively observed in Figure 7, which shows the first doses for 2, 3, and 5  $\mu\text{m}$  circles that exhibit a smooth surface across the majority of the bottom of the cylindrical wells. This is also the crossing point for the horizontal and vertical lines in Figure 6. Notable features of these dose-to-clear structures are the smooth, nearly vertical sidewalls, as opposed to the underexposed structures seen in Figure 5. It is also important to note that these structures still show roughness, due to the slightly uneven surface of the resist, around the edges. Though it is not as extreme as the grass or the rough sidewalls seen in Figure 5a-c, this could be remedied by a descum step. This roughness also decreases for the over-exposed structures, so if smooth surfaces is more important than exact diameter, that is an option.

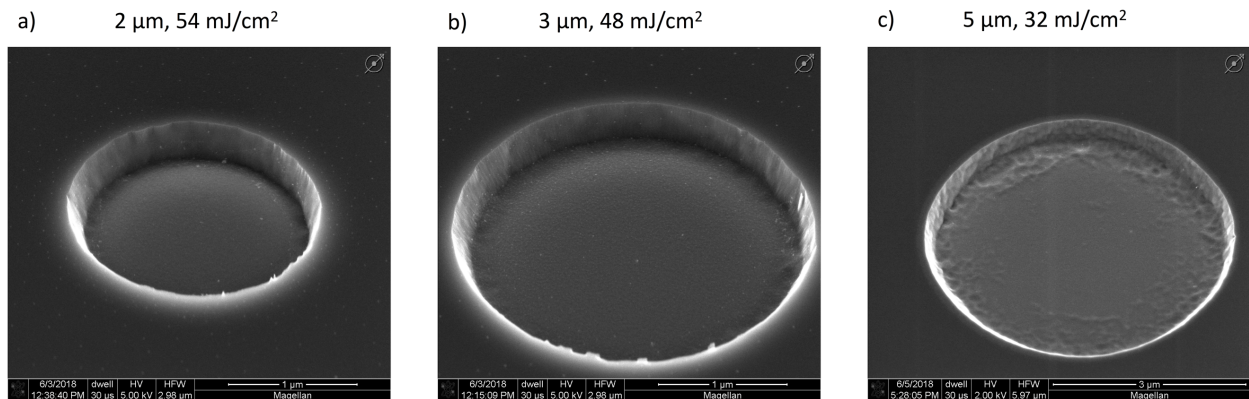


Figure 8: Dose-to-clear and closest to nominal radius

### ***Grayscale pattern etching***

The final aspect of our project was grayscale pattern transfer of a chiral metamaterial. Figures 8 and 9 show the results of this effort. We patterned 5 and 10  $\mu\text{m}$  diameter circles, giving each third of the circle a different grayscale value. We did this for three different maximum

grayscale doses, 512, 712, and 912  $\text{mJ}/\text{cm}^2$ . We then did one 20-nm descum before etching for 500 s. We chose not to bake on this step, due to concerns over reflow eliminating the grayscale topography. For this reason, we see some grass and sidewall roughness in our final structures, but as evidenced by our previous optimization, it is possible to eliminate issues.

From this dose test, shown in Figure 9, we found that the base dose of 712  $\text{mJ}/\text{cm}^2$  gave us the highest grayscale contrast in both the 5 and 10  $\mu\text{m}$  diameter circles (see caption for exact doses used). For the lower doses, the contrast between the top left (lowest dose for each circle) and top right (middle dose for each circle) are minimal. For the higher doses, the contrast between the top right and the bottom (highest dose for each circle) are also very small. Figure 9 shows part of an array of the 10  $\mu\text{m}$  circles using the base dose of 712  $\text{mJ}/\text{cm}^2$ .

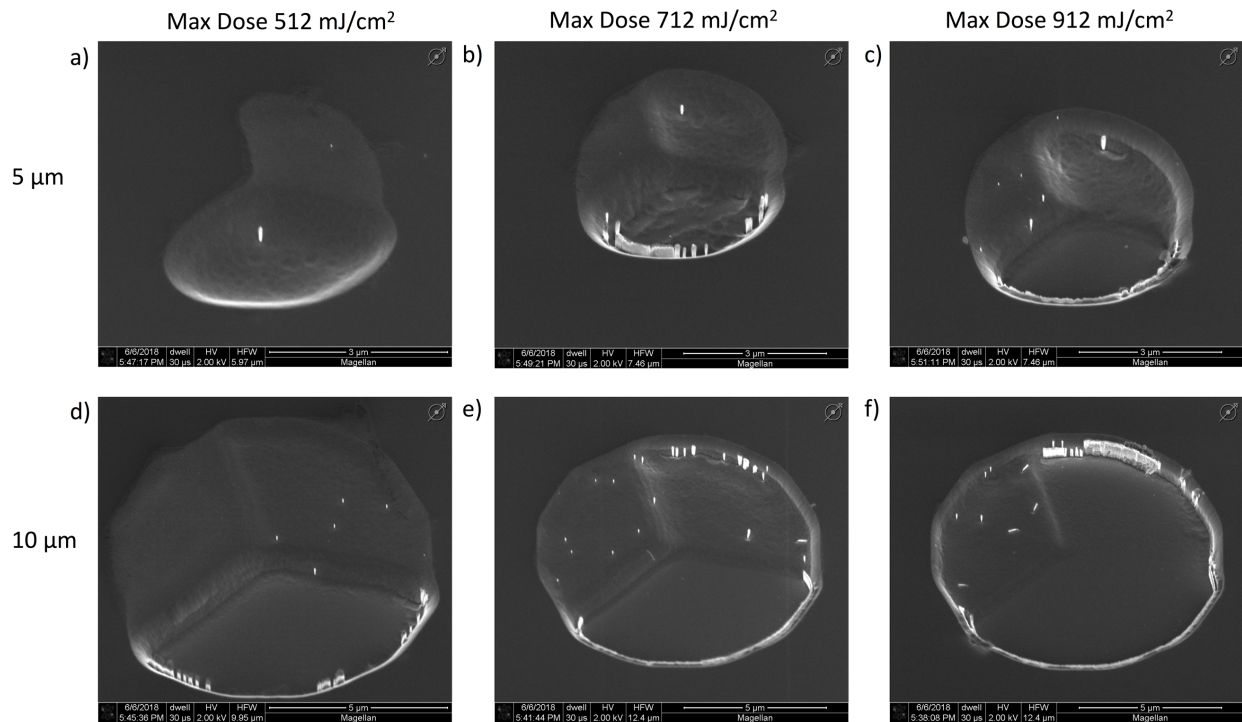


Figure 9: SEMs of chiral structures taken at a  $40^\circ$  angle. 5  $\mu\text{m}$  diameter circles were etched with a base dose of a) 512  $\text{mJ}/\text{cm}^2$  with gray values of 7, 12, and 20, giving final doses of 15, 24, and 40  $\text{mJ}/\text{cm}^2$ , b) 712  $\text{mJ}/\text{cm}^2$  with gray values of 7, 12, and 20, giving final doses of 19, 33, and 55 and c) 912  $\text{mJ}/\text{cm}^2$  with gray values of 7, 12, and 20, giving final doses of 25, 43, and 71. 10  $\mu\text{m}$  diameter circles were etched with a base dose of d) 512  $\text{mJ}/\text{cm}^2$  with gray values of 10, 15, and 30, giving final doses of 20, 30, and 60  $\text{mJ}/\text{cm}^2$ , e) 712  $\text{mJ}/\text{cm}^2$  with gray values of 10, 15, and 30, giving final doses of 28, 42, and 83 and f) 912  $\text{mJ}/\text{cm}^2$  with gray values of 10, 15, and 30, giving final doses of 36, 53, and 107.

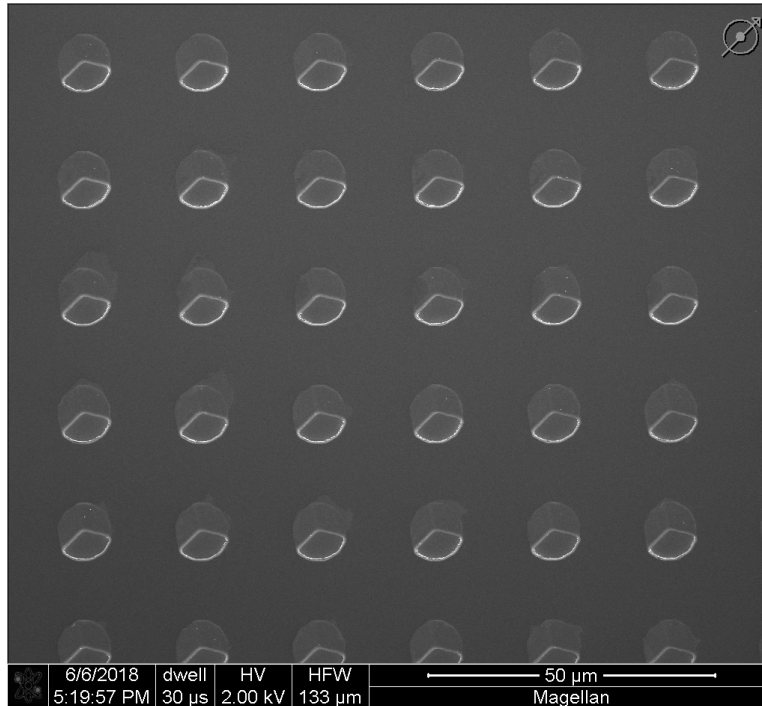


Figure 10: SEM of an array of grayscale 10  $\mu\text{m}$  diameter circles, with visible variation in dose in the thirds of the circle (shallowest etch on top left, middle depth on top right, and deepest etch on bottom).

## **Conclusion**

We determined grayscale dose curves for 1 and 1.6  $\mu\text{m}$  Shipley 3612 resist on silicon wafers for non-resolution limited features using the Nanospec and S-neox, and characterized the sidewalls of these features. Notably, the sidewalls are significantly angled at low doses, spanning a width of roughly 500 nm, a significant value for the resolution-limited features in this project. We exposed near-resolution limited circles (2-5  $\mu\text{m}$  in diameter) in the Heidelberg using 1  $\mu\text{m}$  thick Shipley 3612 resist and transferred those patterns into the underlying silicon, gathering data about the effects of dose variation in resolution limited features. Our pattern transfer was optimized when using a 2 hr post bake in a 110°C oven, and a 20 nm UV-ozone descum at 100°C. We characterized the parabolic nature of low-dose small features after the etch, observed a diameter change with dose, and variation in dose-to-clear depending on the structure size. Finally, we used our 1  $\mu\text{m}$  grayscale dose curve to pattern a 5 and 10  $\mu\text{m}$  grayscale chiral metamaterial, which could be of use at terahertz frequencies.

## **Acknowledgements**

Many thanks to our mentors Swaroop and Andrew; Uli, Usha, and Mahnaz for training; Roger and Mary for coordinating the course; and the rest of the staff, mentors, and class members for feedback throughout the quarter.

## **References**

[1] Zhang, Shuang, et al. "Negative refractive index in chiral metamaterials." *Physical review letters* 102.2 (2009): 023901.